



Coherent anti-Stokes Raman scattering and two photon excited fluorescence for neurosurgery



Bernd F.M. Romeike^{a,*}, Tobias Meyer^b, Rupert Reichart^c, Rolf Kalff^c, Iver Petersen^a, Benjamin Dietzek^{b,d}, Jürgen Popp^{b,d}

^a Institute of Pathology, Jena University Hospital, Friedrich-Schiller-University, Erlanger Allee 101, D-07740 Jena, Germany

^b Institute of Photonic Technology (IPHT) Jena e.V., Albert-Einstein-Straße 9, D-07745 Jena, Germany

^c Clinic for Neurosurgery, Jena University Hospital, Friedrich-Schiller-University, Erlanger Allee 101, D-07740 Jena, Germany

^d Institute of Physical Chemistry and Abbe Center of Photonics, Friedrich-Schiller-University Jena, Helmholtzweg 4, D-07743 Jena, Germany

ARTICLE INFO

Article history:

Received 25 October 2014

Received in revised form 3 January 2015

Accepted 25 January 2015

Available online 31 January 2015

Keywords:

Brain tumors

Coherent anti-Stokes Raman scattering (CARS)

Intraoperative imaging

Molecular imaging

Two photon excited fluorescence (TPEF)

ABSTRACT

Objective: There is no established method for *in vivo* imaging during biopsy and surgery of the brain, which is capable to generate competitive images in terms of resolution and contrast comparable with histopathological staining.

Methods: Coherent anti-Stokes Raman scattering (CARS) and two photon excited fluorescence (TPEF) microscopy are non-invasive all optical imaging techniques that are capable of high resolution, label-free, real-time, nondestructive examination of living cells and tissues. They provide image contrast based on the molecular composition of the specimen which allows the study of large tissue areas of frozen tissue sections *ex vivo*.

Results: Here, preliminary data on 55 lesions of the central nervous system are presented. The generated images very nicely demonstrate cytological and architectural features required for pathological tumor typing and grading. Furthermore, information on the molecular content of a probe is provided. The tool will be implemented into a biopsy needle or endoscope in the near future for *in vivo* studies.

Conclusion: With this promising multimodal imaging approach the neurosurgeon might directly see blood vessels to minimize the risk for biopsy associated hemorrhages. The attending neuropathologist might directly identify the tumor and guide the selection of representative specimens for further studies. Thus, collection of non-representative material could be avoided and the risk to injure eloquent brain tissue minimized.

© 2015 Elsevier B.V. All rights reserved.

1. Introduction

Label free intravital microscopy holds great promise to improve tissue sampling, *i.e.* reducing the risk of procuring non-representative specimens, and minimizing the risk of bleeding by visualization and avoiding destroying blood vessels, especially during stereotactic surgery or other minimal invasive central nervous system surgery. Furthermore, where applicable, neurosurgeons could be guided to borders of lesions for exact orientation and to avoid excessive resection of functional or eloquent brain tissue during surgery by precise boundary detection.

* Corresponding author at: Institute of Pathology, Neuropathology Section, Jena University Hospital, Friedrich Schiller University, Erlanger Allee 101, D-07747 Jena, Germany. Tel.: +49 3641 9 3247 55; fax: +49 3641 9 3247 52.

E-mail address: bernd.romeike@med.uni-jena.de (B.F.M. Romeike).

Especially, the application of coherent anti-Stokes Raman scattering (CARS) [1] and tissue intrinsic two photon excited fluorescence (TPEF) [2] microscopy are promising tools which enable intraoperative imaging of histological structures without staining the tissue. The generated images provide a detailed insight into the molecular composition of the sample. CARS is widely used for visualizing the distribution and concentration of lipids [3], while TPEF enables displaying the spatial distribution of autofluorescing molecular species like elastin, keratin or NAD(P)H [4], thus offering molecular selective imaging. The techniques allow for spatially highly resolved imaging even of single cells. The penetration depth in tissue is a few 100 μm which would provide a sufficient security margin for intraoperative guidance in order to avoid damaging functional structures, *e.g.* blood vessels. The pulsed illumination in nonlinear imaging allows investigation of the sample at low average power thus avoiding photodamage of the tissue but providing good image contrast.

In vivo CARS imaging has already been demonstrated even at video rate and proved especially valuable in displaying the distribution of lipids [5]. This makes CARS especially interesting for the study of lipid rich brain tissue. However, for *in vivo* applications the technology has to be safe and non-destructive. Cell line and animal studies could so far show that CARS application *in vivo* is safe with no or negligible photodamage [6,7]. CARS microscopy has been successfully used *ex vivo* to image mice brain [8,9] and various tumors, among them also brain tumors [8,10–12]. CARS was also combined with further imaging techniques on small sets of samples [13].

Here, we present preliminary data from a systematic study on a set of various specimens from the central nervous system *ex vivo* in order to exploit the potential of a combination of CARS and TPEF for multimodal *in vivo* imaging and to determine possible limitations.

2. Materials and methods

2.1. Materials

We prospectively collected consecutive brain biopsy specimens of patients operated at the Clinic for Neurosurgery, Jena University Hospital with the permission of the ethics committee. Informed

consent for experimentation was obtained by all patients. For diagnostic work-up all specimens were submitted to a special trained neuropathologist (BFMR), where applicable pathological typing and grading of the specimens was performed according to the current World Health Organization (WHO) Classification of Tumors of the Central Nervous System [14]. Intraoperative diagnosis was based on giemsa stained cytological smear preparations and hematoxylin and eosin (H&E) stained cryostat sections. Final diagnoses were confirmed by standard formalin fixed paraffin embedded tissue with standard stains including immunohistochemical methods.

Unstained parallel sections of the diagnostic cryostat sections were subject to CARS, and TPEF. Sections were transferred onto calcium fluoride slides and air dried under ambient conditions. For definite comparison besides the intraoperative parallel cryostat section also the original air dried sections were later stained with hematoxylin and eosin after completion of CARS and TPEF imaging. The studied areas were again searched on the slides and compared to CARS and TPEF images. These areas were again compared with the parallel areas of the initial diagnostic intraoperatively made H&E cryostat section which was then documented and compared with CARS and TPEF images as shown in Figs. 1 and 2.

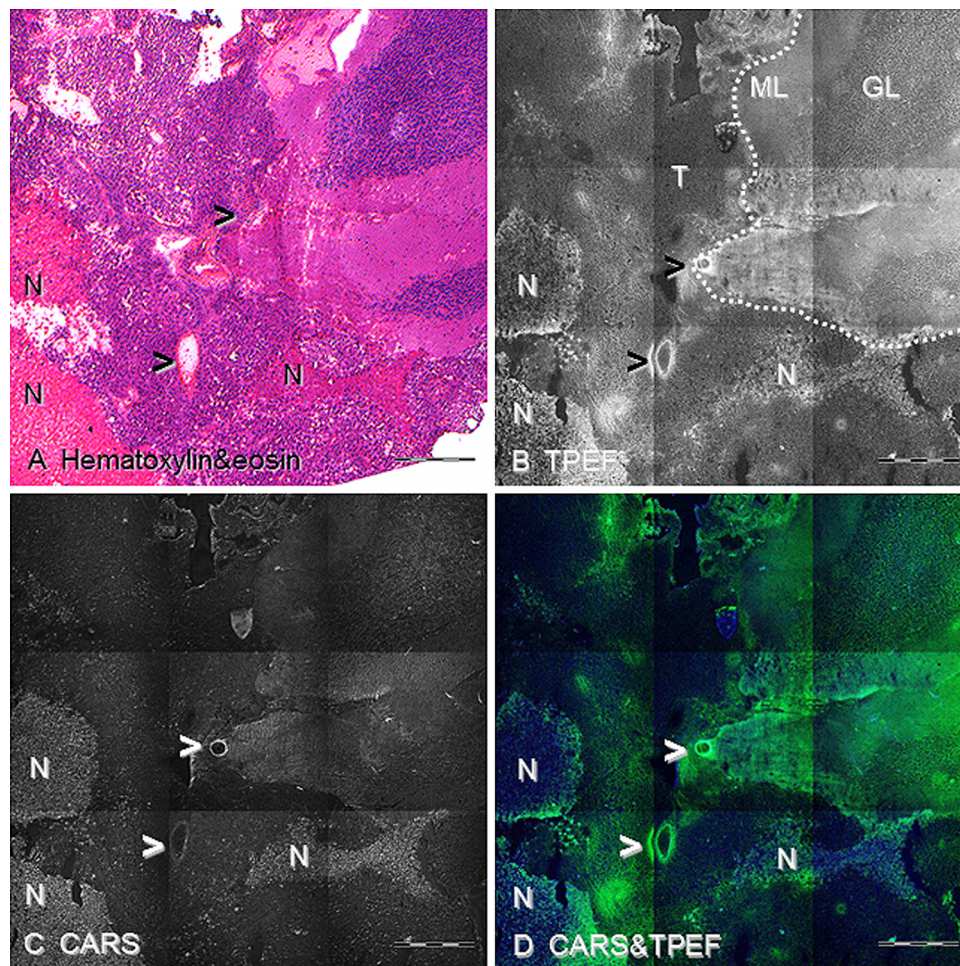


Fig. 1. Low magnification of a cerebellar metastasis of a small cell lung carcinoma, image size 3 mm × 3 mm. (A) Hematoxylin and eosin (H&E) stain shows preexisting cerebellar cortex (upper right), blood vessels (>), tumor and necroses (N). Especially blood vessels are easily detected, even without much experience. (B) The TPEF image highlights the autofluorescing spectrum of preexisting cerebellar molecular layer (ML) and granular layer (GL) vital tumor (T), and necrotic areas (N). There is a clear border between tumor and cerebellum (dotted line). Necrotic tissue contains fluorescing spectrum originating from tissue degradation. (C) Also on the CARS image the cerebellar cortex is sharply demarcated from tumor due to the relative lipid deficiency in tumor tissue with respect to normal brain tissue. Necrotic areas (N) are highlighted indicating higher lipid content and enabling clear differentiation from vital tumor. (D) Combination of CARS and TPEF images. H&E stain (A), TPEF (B), CARS at 2850 cm⁻¹(C) and combined multimodal CARS-TPEF-imaging (D) displaying CARS in blue and TPEF in green. Scale bar 500 μm. (For interpretation of the references to color in this figure legend, the reader is referred to the web version of this article.)

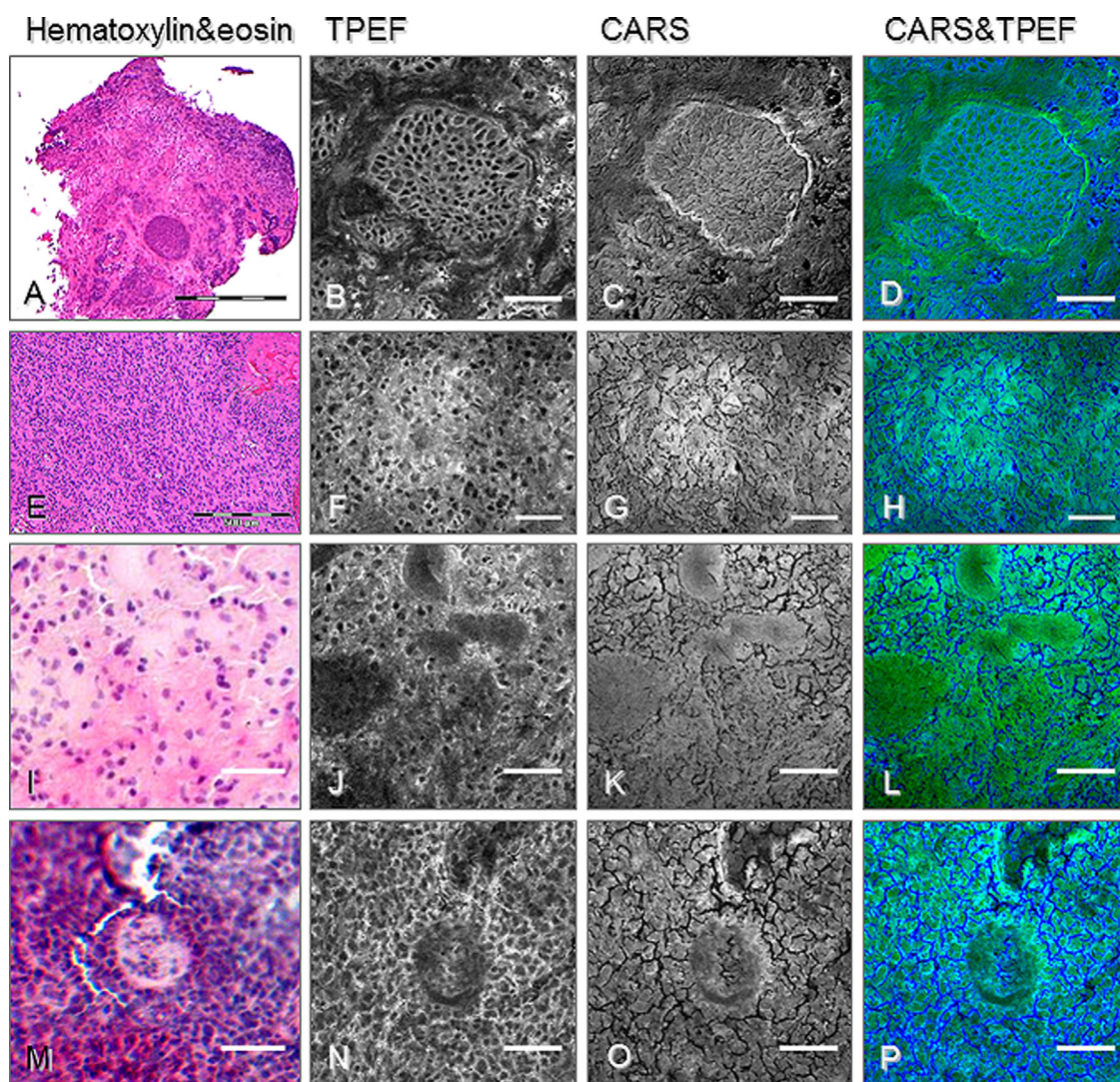


Fig. 2. H&E stained overview images of various tumors and higher magnifications of multimodal nonlinear images of parallel tissue sections. In the first column H&E stained section are depicted, whereas in the second column TPEF-, in the third CARS- and in the fourth combined CARS (green) and TPEF (blue) – images are shown. (A–D) In the first row a brain metastasis of a squamous cell carcinoma is shown. CARS and TPEF highlight the boundaries and the architecture (B–D). The second row contains in panels E–H images of a diffuse glioma with moderate cellularity. Panels I–L show the outer border, *i.e.* diffuse manifestation of a lymphoma whereas images (M–P) show an area of the same lymphoma with high cell density. Especially TPEF allows for easy identification of variability in cell density in different areas. Scale bars (A) and (E): 500 μm , all others: 50 μm . (For interpretation of the references to color in this figure legend, the reader is referred to the web version of this article.)

2.2. CARS and TPEF

The setup used for combined CARS and TPEF imaging of brain tissue sections is based on a previously reported setup [13]. A Ti:Sa laser (Mira HP, Coherent, USA) emits laser pulses of 2 ps pulse duration, 76 MHz repetition rate and 3 W average power at 830 nm. One part of the laser output is used to pump an optical parametric oscillator (OPO, APE, Germany) for generating the CARS pump wavelength at 670 nm. The other fraction of the Ti:Sa-laser is used as Stokes laser for generating the CARS process. The output of the OPO at 670 nm and of the Ti:Sa at 830 nm are spatially and temporally recombined by a mechanical delay and a dichroic mirror and directed to the entrance port of a confocal laser scanning microscope consisting of a Axiovert 200M microscope equipped with a scanning module LSM 510 (both Zeiss, Germany). The CARS signal is spectrally separated from the exciting lasers by a stack of short- and bandpass filters (3rd millennium, Omega Optical, USA) and detected by a photomultiplier module in forward direction, whereas the TPEF signal is collected by the objective in backward direction and separated by a set of dichroic mirrors and filters

(Zeiss, Germany) and detected by a photomultiplier tube (PMT) module. The schematic layout of the setup is depicted in Fig. 3, while the principle processes for signal generation will be briefly described in the following. TPEF – in contrast to single photon fluorescence – is excited by the simultaneous absorption of two low energy photons. The molecule relaxes and emits a photon when returning to its electronic ground state. The scheme of the process is depicted in Fig. 3(B). Since only certain molecules emit fluorescence light, TPEF is limited to display the spatial distribution of such molecular signatures. In tissue abundant autofluorophors include keratin, elastin, NADPH, melanin and tryptophan. By choosing appropriate excitation and emission spectral windows, the contribution of different signatures can be disentangled. Here the emission between 435 and 485 nm was detected. TPEF especially allows for visualizing the cell nuclei, since fluorescing signatures are mainly located in the cytoplasm, leading to a sharp contrast at the nuclear membrane (Figs. 1 and 2).

The second imaging method, CARS, requires two synchronized lasers for sample illumination. When the difference in frequency of both lasers matches a vibrational resonance, this level becomes

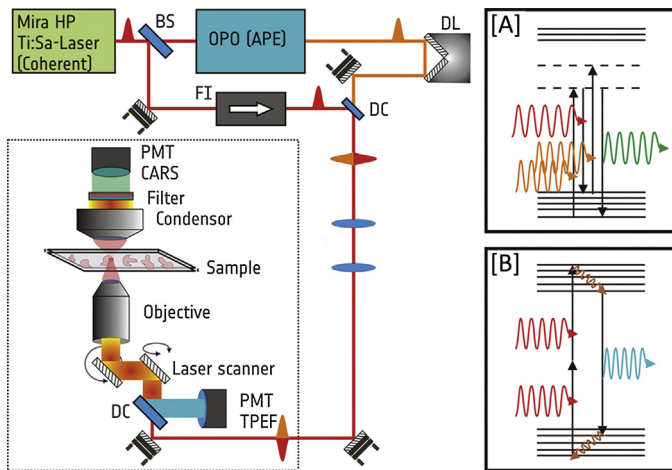


Fig. 3. Diagrammatic layout of the microscopic setup used for simultaneous two photon excited fluorescence (TPEF) and coherent anti-Stokes Raman scattering (CARS) imaging. The emission and excitation schemes of these processes are depicted in the insets (A, CARS) and (B, TPEF). A Ti:Sa laser Mira HP (coherent) is used for illumination. A fraction is split by a beamsplitter BS for pumping an optical parametric oscillator (OPO, from APE), which allows for continuous tuning of the CARS-pump wavelength from 500 to 1600 nm. The other fraction serves as fixed wavelength Stokes beam or excitation laser for TPEF. A Faraday isolator (FI) suppresses backreflections from the microscope. For CARS a delay line (DL) temporally overlaps pump- and Stokes pulses and corrects for different dispersion of both colors in the optical path. Both lasers are recombined using a dichroic mirror (DC). Then the lasers enter a commercial laser scanning microscope (Zeiss). Photomultiplier modules (PMT), filters and dichroic beamsplitters (DC) are used to separate TPEF and CARS signals from the excitation lasers. In (A) the CARS process is displayed. Pump- and Stokes photons coherently populate an excited vibrational level. Coherent Raman scattering from this excited level results in the emission of directional laser-like CARS radiation. In TPEF (B) two photons are simultaneously absorbed to electronically excite the molecule, which then spontaneously relaxes into the electronic ground state by fluorescence emission.

populated and further photons of the pump laser are inelastically scattered off this resonance, generating the signal at the anti-Stokes frequency. Since the emission is at shorter wavelength with respect to the illumination lasers, there is no interference with single photon fluorescence as in conventional Raman scattering techniques. The basic scattering process is depicted in Fig. 3(A). For CARS imaging the aliphatic C–H-stretching vibration at 2850 cm^{-1} was chosen in order to visualize the distribution and concentration of lipids. This resonance is especially informative, since brain tissue is extremely rich in lipids in comparison to other types of tissue, while the lipid concentration in tumors is usually lower; hence, imaging in this resonance with the CH stretching band allows differentiating cancerous from brain tissue [8,13]. For a histopathological application, two aspects are important for imaging. First, the technique needs to be applicable to a large enough tissue area, preferably of several mm in diameter, and allow for fast imaging acquisition. For this purpose a $10\times$ objective has been used, which offers a field of view of $1.2\text{ mm} \times 1.2\text{ mm}$. By merging up to 15×15 images tissue areas of $15\text{ mm} \times 15\text{ mm}$ can be investigated. However, area imaging of this size is time consuming. At maximum resolution 30 s are required for a single image of decent signal to noise ratio, which would result in image acquisition times of almost 2 h for the largest possible mosaics. Meanwhile lower resolution mosaics can be acquired within a few minutes allowing for determining large scale tissue boundaries. For resolving the cellular morphology and cellular or nuclear atypia a higher magnification $20\times$ objective has been used, allowing visualizing single cells and cell nuclei. Thereby important parameters for tumor grading like nucleus to cytoplasm ratio, cell density, nuclear size and shape can be determined by CARS and TPEF images [15].

3. Results

In total, 55 intracranial lesions were studied. Neuropathological diagnoses were metastatic carcinoma ($N=15$), meningioma ($N=10$), glioblastoma ($N=6$), other diffuse gliomas ($N=7$), brain tissue with gliotic/reactive changes ($N=5$), pituitary adenoma ($N=3$), soft tissue not otherwise specified ($N=3$), lymphoma ($N=2$) and schwannoma ($N=2$).

In all cases vessels were easily recognized and with little experience many architectural features could be visualized. For an experienced neuropathologist the images generated by CARS and TPEF allowed even the identification of smaller and more specific anatomic structures almost comparable to H&E stained cryostat sections (Figs. 1 and 2). Furthermore, information of the molecular composition of the tissue was provided. The contrast between nuclei, cytoplasm and cell borders or surrounding tissue differs between glioma and lymphoma. CARS images at the CH-stretching vibration at 2850 cm^{-1} showed a very pronounced signal indicating a great amount of fatty acids, which give rise to the intense CARS signal.

In order to determine the tissue's cell density TPEF images were recorded with lasers for excitation at 670 and 830 nm for better visualizing cell nuclei. The fluorescence signal was detected in the range between 435 and 485 nm. Hence, the second harmonic generation (SHG) signal of both lasers at 413 and 335 nm, i.e. twice the photon energy of the incident laser light, was spectrally filtered and excluded in these images. The TPEF images show single cell nuclei by negative contrast (Fig. 2(B), (F), (J) and (N)). White matter can be differentiated from gray matter and tumor tissue (Fig. 1(C)).

4. Discussion

We evaluated the suitability of multimodal nonlinear imaging for potential intra-operative visualization of intracranial lesions. The combination of CARS and TPEF images provide pathologists and neurosurgeons with very useful information. With no labeling the described method is capable to deliver detailed histomorphological pictures. As the images show, for an experienced pathologist the observable morphologic details would be sufficient for assessment for typing and grading of a lesion if successfully reproduced *in vivo*. Necroses are obviously highlighted, probably due to a higher lipid or cholesterol content [16]. This – however – is not only useful for grading of diffuse gliomas. Also the biopsy of non-representative necrotic areas of lesions can be omitted. On the other hand, representative specimens can be taken under direct vision. An experienced pathologist will not face greater problems concerning the interpretation of CARS as well as TPEF images. In the future the technique might be applied not only *ex vivo* but also *in vivo* in the operating theater. No sample preparation or staining or other tissue manipulation will be necessary. For the application of this method the pathologist should be in the operating room and look there at the images together with the neurosurgeon. It seems not advisable, to let the neurosurgeon alone with multimodal nonlinear imaging. A major advance would be the visualization of blood vessels before they get injured. This obstacle seems feasible as the fibers of the vessel walls give a strong contrast to the surrounding brain tissue with high fat content. Furthermore, heme is strongly absorbing, leading to a greatly reduced TPEF signal within blood vessels. Thus an accidental injury of blood vessels might be avoided and the risk of surgery related blood loss and hemorrhages might be reduced. However, the described technique will not replace but complement established intraoperative neuronavigation systems.

Especially the risk of stereotactic or other very small/little biopsies might be lowered because only what is really needed

to establish the diagnosis is taken out under direct vision. Non-representative specimens of the tumor surrounding and necroses are omitted. Diagnostically unnecessary tissue is left in place and the actual biopsy material is kept to a minimum.

Furthermore, eventual borders between the pathological process and the brain can be identified. Determining the borders of a tumor will eventually improve the accomplishment of as complete as possible tumor removals.

At the end, there will be no additional time effort because the time for the visual inspection of excised tissue can be spared in omitting taking non-representative biopsy specimens in the vicinity of the actual lesion.

It has been previously shown, that the method of CARS can be applied securely *in vivo* [6,7]. The method is expected to complement established methods in biomedical and diagnostic applications. In single selected cases it might even be possible to omit a biopsy because the visualization of the pathological process suffices if there is no need for tissue for further pathological, microbiological or molecular genetic studies.

5. Future trend: miniaturization

As CARS images can be recorded at video rate live imaging is possible [5]. For a useful clinical application it will be necessary to miniaturize CARS microscopy, e.g. develop miniaturized fiber lasers [17]. Recent work has focused on developing even endoscopic systems [18–21]. Also our group works on miniaturization.

6. Conclusion

CARS and TPEF imaging could aid the neurosurgeon in guiding in order to minimize the risk to injure eloquent brain tissue and to minimize the risk to unintentional injury of blood vessels, thus reducing biopsy associated blood loss, hemorrhages and strokes. An experienced neuropathologist could identify types of lesions, eventually including tumor grading and aid during the selection of representative specimens, thus avoiding collection of non-representative material. This technique will require close cooperation between neurosurgeons and neuropathologists.

Acknowledgements

Financial support from European Union via the 'Europäischer Fonds für Regionale Entwicklung (EFRE)' and the 'Thüringer Ministerium für Bildung Wissenschaft und Kultur (TMBWK)' (projects: B578-06001, 14.90 HWP and B714-07037), via the German Science Foundation (Jena School of Microbial Communication) and

the German Federal Ministry for Science and Education (BMBF) *MediCARS* (FKZ: 13N10774) is gratefully acknowledged.

References

- [1] Zumbusch A, Holtom GR, Xie XS. Three-dimensional vibrational imaging by coherent anti-Stokes Raman scattering. *Phys Rev Lett* 1999;82:4142–5.
- [2] Zipfel WR, Williams RM, Christie R, Nikitin AY, Hyman BT, Webb WW. Live tissue intrinsic emission microscopy using multiphoton-excited native fluorescence and second harmonic generation. *Proc Natl Acad Sci U S A* 2003;100:7075–80.
- [3] Evans CL, Xie XS. Coherent anti-stokes Raman scattering microscopy: chemical imaging for biology and medicine. *Annu Rev Anal Chem (Palo Alto, CA)* 2008;1:883–909.
- [4] Huang S, Heikal AA, Webb WW. Two-photon fluorescence spectroscopy and microscopy of NAD(P)H and flavoprotein. *Biophys J* 2002;82:2811–25.
- [5] Evans CL, Potma EO, Puoris'haag M, Cote D, Lin CP, Xie XS. Chemical imaging of tissue *in vivo* with video-rate coherent anti-Stokes Raman scattering microscopy. *Proc Natl Acad Sci U S A* 2005;102:16807–12.
- [6] Fu Y, Wang H, Shi R, Cheng JX. Characterization of photodamage in coherent anti-Stokes Raman scattering microscopy. *Opt Express* 2006;14:3942–51.
- [7] Nan X, Potma EO, Xie XS. Nonperturbative chemical imaging of organelle transport in living cells with coherent anti-stokes Raman scattering microscopy. *Biophys J* 2006;91:728–35.
- [8] Evans CL, Xu X, Kesari S, Xie XS, Wong ST, Young GS. Chemically-selective imaging of brain structures with CARS microscopy. *Opt Express* 2007;15:12076–87.
- [9] Fu Y, Huff TB, Wang HW, Wang H, Cheng JX. *Ex vivo* and *in vivo* imaging of myelin fibers in mouse brain by coherent anti-Stokes Raman scattering microscopy. *Opt Express* 2008;16:19396–409.
- [10] Le TT, Rehrer CW, Huff TB, Nichols MB, Camarillo IG, Cheng JX. Nonlinear optical imaging to evaluate the impact of obesity on mammary gland and tumor stroma. *Mol Imaging* 2007;6:205–11.
- [11] Vogler N, Meyer T, Akimov D, Latka I, Krafft C, Bendsoe N, et al. Multimodal imaging to study the morphochemistry of basal cell carcinoma. *J Biophotonics* 2010;3:728–36.
- [12] Krafft C, Ramoji AA, Bielecki C, Vogler N, Meyer T, Akimov D, et al. A comparative Raman and CARS imaging study of colon tissue. *J Biophotonics* 2009;2:303–12.
- [13] Meyer T, Bergner N, Bielecki C, Krafft C, Akimov D, Romeike BF, et al. Nonlinear microscopy, infrared, and Raman microspectroscopy for brain tumor analysis. *J Biomed Opt* 2011;16:021113.
- [14] Louis DN, Ohgaki H, Wiestler OD, Cavenee WK. WHO classification of tumours of the central nervous system. 4th ed. Lyon: IARC Press; 2007.
- [15] Medyukhina A, Meyer T, Schmitt M, Romeike BF, Dietzek B, Popp J. Towards automated segmentation of cells and cell nuclei in nonlinear optical microscopy. *J Biophotonics* 2012;5:878–88.
- [16] Koljenovic S, Choo-Smith LP, Bakker Schut TC, Kros JM, van den Berge HJ, Puppels GJ. Discriminating vital tumor from necrotic tissue in human glioblastoma tissue samples by Raman spectroscopy. *Lab Invest* 2002;82:1265–77.
- [17] Baumgartl M, Chemnitz M, Jauregui C, Meyer T, Dietzek B, Popp J, et al. All-fiber laser source for CARS microscopy based on fiber optical parametric frequency conversion. *Opt Express* 2012;20:4484–93.
- [18] Wang H, Huff TB, Cheng JX. Coherent anti-Stokes Raman scattering imaging with a laser source delivered by a photonic crystal fiber. *Opt Lett* 2006;31:1417–9.
- [19] Legare F, Evans CL, Ganikhanov F, Xie XS. Towards CARS endoscopy. *Opt Express* 2006;14:4427–32.
- [20] Wang H, Huff TB, Fu Y, Jia KY, Cheng JX. Increasing the imaging depth of coherent anti-Stokes Raman scattering microscopy with a miniature microscope objective. *Opt Lett* 2007;32:2212–4.
- [21] Balu M, Liu G, Chen Z, Tromberg BJ, Potma EO. Fiber delivered probe for efficient CARS imaging of tissues. *Opt Express* 2010;18:2380–8.